JOURNAL OF APPLIED ELECTROCHEMISTRY **27** (1997) 1052–1060

Electrocatalytic oxidation of methanol on platinum nanoparticles electrodeposited onto porous carbon substrates*

F. GLOAGUEN, J.-M. LÉGER, C. LAMY

Laboratoire de Chimie I, Electrochimie et Interactions, URA au CNRS no. 350, Université de Poitiers, 40 av. du Recteur Pineau, 86022 Poitiers, France

Received 30 September 1996; revised 24 December 1996

To achieve methanol fuel cell electrodes allowing a high catalyst use, thin layers of various carbon powders and recast Nafion® were electrochemically plated with platinum. The resulting Pt deposits were characterized by hydrogen and carbon monoxide electrosorption, as well as by transmission electron microscopy. Methanol oxidation was then carried out using cyclic voltammetry. The influence of the amount of carbon surface oxides and the effect of Pt specific surface area on the Pt catalytic activity were thus investigated.

Keywords: *methanol oxidation, TEM, carbon support, platinum catalyst, particle size effect*

1. Introduction

Methanol oxidation is of great importance in fuel cell technology, namely in the direct methanol fuel cell (DMFC) aimed to power electric vehicles. However, direct electrooxidation is a very complex reaction because many intermediate species are involved. In acid medium this reaction requires platinum-based catalysts, even though Pt exhibits a rather low activity [1].

To decrease the amount of Pt at the methanol anode, the electrocatalyst is usually dispersed on carbon supports *via* chemical [2] or electrochemical [3] reduction of Pt salts. Beyond that, in the case of a DMFC with a proton exchange membrane, the active layer generally consists of carbon supported catalysts and recast Nafion® [4]. To enhance the catalyst use, accessibility of the reactant to the catalytic sites, as well as electronic contact with the current collector must be optimized [4, 5]. On the one hand, it was claimed [6, 7] that electrochemical reduction of cationic salts, such as $[Pt(NH_3)_4]^{2+}$, within a porous electrode consisting primarily of carbon powder and recast Nafion®, provides Pt catalytic sites efficiently used. However, other authors [8] found that the kinetics of the electrochemical reduction of $[Pt(NH_3)_4]^{2+}$ is very slow, even on a Pt electrode (i.e., in the case of a non epitaxic growth). On the other hand, $PtCl_6^{2-}$ is able to diffuse through a thin film of Nafion®, although the latter is a cation exchange polymer. The reduction kinetics of this Pt salt at the carbon/recast Nafion® interface is, moreover, fast [9, 10]. As a result, the electrochemical reduction of $PtCl_6^{2-}$ within a film consisting of carbon powder plus Nafion® should provide active layers with well dispersed catalytic sites. The characterization of such active layers by electrochemical measurements and direct observations at the micrometric scale is reported in the present work.

The second part of this paper is concerned with the kinetics of electrochemical reactions at dispersed electrodes. It is well-known that a large increase of the specific surface area (i.e., the surface area to mass ratio), usually associated with a particle size decrease, can modify the catalytic activity [11]. On one hand, a so-called particle size effect was reported for the oxygen reduction reaction (ORR) at supported Pt electrocatalysts [12]; with decreasing particle size, the observed lower activity was ascribed to a stronger adsorption of oxygenated species [13, 14]. On the other hand, the effect of Pt specific surface area on the methanol oxidation kinetics was also investigated, but the results led to more contradictory conclusions [15, 16]. Although the catalytic activity usually decreases at high Pt specific surface areas [13, 17, 18], the amount of oxide groups on the carbon surface also modifies the kinetics [18, 19]. Concerning the electrooxidation of methanol, the following two factors have also to be considered. First, many intermediate species are involved and some of these act as 'poisons' (e.g., CO [20] which comes from the dissociative adsorption of methanol at low potentials). Hence, not only the adsorption energy of oxygenated species (i.e., a similar effect as for the ORR), but also the adsorption energy of 'poisoning' and reactive intermediates may depend on the specific Pt area. Second, the crystallographic structure of the Pt surface plays a key role in the oxidation of methanol [21]

* This paper is dedicated to Professor Roger Parsons on the occasion of his 70th birthday.

0021-891X

and formic acid [22], but not for the ORR [23]. Related to the Pt specific surface area, modifications of the surface structure may accordingly change the amount of initially adsorbed methanol, as well as the surface distribution of reactive and poisoning species.

The purpose of this paper is twofold: first, to determine the characteristics of Pt electrodeposited on various carbon supports mixed with recast Nafion®, and second, to investigate the effect of the amount of carbon surface oxides, as well as the influence of the Pt specific surface area, on the methanol oxidation at various carbon supported Pt/recast Nafion® interfaces. Accurate measurements of the specific surface area are necessary to obtain experimental evidence for the so-called particle size effect. The electrode must also have a well-defined geometry. In this work, the Pt electrodeposits are characterized by transmission electron microscopy (TEM), as well as by hydrogen and carbon monoxide electrosorption. For kinetic measurements, a compact thin layer of carbon powder, recast Nafion® and electrochemically dispersed Pt is used. This method [24] provides an electrode geometry, more easily reproducible than the geometry of liquid flooded electrodes used in some previous kinetic studies. It is also to be noticed that Nafion® (1100 EW) has well-defined properties, as a polymer electrolyte; the adsorption energy of sulfonate ions on Pt is a little lower than that of the sulfate ions, but stronger than that of the perchlorate ions [25].

2. Experimental details

2.1. *Reagents and electrodes*

Solutions were prepared from H_2SO_4 (Suprapur, Merck), K_2PtCl_6 (Alfa) and CH_3OH (pro analysi, Merck). Ultrapure water (Milli-Q system, Millipore) was used for all purposes. The 1100 EW Nafion® was recast from a 5 wt % solution (Aldrich). The sulfate concentration in solution was limited to 0.1 M, to decrease the entrance of sulfate anions into the recast Nafion® phase during the electrochemical experiments, because the Donnan potential difference decreases the amount of anions within the membrane compared to the amount in solution, since the solution is diluted.

The catalyst supports were either a graphite powder (HSAG 300, Lonza) or a carbon black (Vulcan XC72, Cabot). The graphite powder HSAG was $300\,m^2\,g^{-1}$ in specific surface area and consisted of stacks with several sheets. Most of the developed area results from basal planes of graphite structure. XRD patterns show thin peaks for the $(0\,0\,2n)$ planes, corresponding to an average d spacing of 0.37 nm [14]. Unfortunately, it was not possible to use the HSAG powder as received, because of metallic and/or organic impurities. Cleaning was achieved by liquid phase oxidation [14] in hot and concentrated nitric acid ($100\,^\circ C, \sim 30$ wt%), for 2 h. The graphite powder was then filtered and thoroughly rinsed with water. The carbon black Vulcan XC72 was about $220\,m^2\,g^{-1}$ in specific surface area. It consisted of small balls (~250 nm in diameter) and presented more irregularities and defects at its surface than the HSAG powder [14]. The Vulcan carbon was used as received or electrochemically oxidized by continuous cycling, from −0.65 to 0.8 V vs a mercury mercurous sulfate electrode (MSE), at $100\,mV\,s^{-1}$ and for 15 min in nitrogen purged 0.1 M H_2SO_4.

A 0.3 cm diameter glassy carbon (GC) stick from Carbone Lorraine, and imbedded in a Teflon rod was used to hold the layer of carbon powder plus recast Nafion®. The GC surface was polished with 0.05 μm alumina powder (Escil A5) and then ultrasonically cleaned in acetone and in water, prior to coating. Measured amounts of carbon powder (~50 mg), Nafion® solution (~1 g) and water (~5 cm^3) were mixed and ultrasonically homogenized. A measured volume (3 to 5 mm^3) of this mixture was then dropped on the GC surface. The solvents were finally evaporated at 80 °C for a few hours.

2.2. *Electrochemical experiments*

The electrochemical equipment included a potentiostat (PAR 362, EG&G), a waveform generator (PAR 175, EG&G), and a *XYt* recorder (LY 1600, Linseis). The electrochemical experiments were carried out at room temperature in a standard two-compartment glass cell. The counter electrode was a glassy carbon sheet. The reference electrode (MSE) was Hg_2SO_4/Hg in saturated K_2SO_4. This electrode, immersed in 0.1 M H_2SO_4, was connected by a Luggin capillary to the working electrode compartment. The potentials are quoted in the MSE scale.

Before each deposition experiments, several voltammograms (from −0.65 to 0.5 V at $20\,mV\,s^{-1}$) were recorded in nitrogen-purged 0.1 M H_2SO_4, both to control the reproducibility of the carbon surface characteristics and to calculate the charge density associated with the double layer of the porous electrode. The platinum electrodeposition was performed by a single potential step in nitrogen-purged and unstirred 0.1 M H_2SO_4 + 2 mM K_2PtCl_6. The potential step (0.05 to −0.5 V) was applied after 1 h of contact with K_2PtCl_6, in order to allow an equilibration of the amount of $PtCl_6^{2-}$ through the recast Nafion® phase [10].

After platinum deposition, the electrode was removed from the deposition solution, thoroughly rinsed with water, and then transferred to a similar cell containing pure 0.1 M H_2SO_4. The hydrogen adsorption coulometry [26], as well as the coulometry of oxidation of a preadsorbed carbon monoxide layer [27], were measured by cyclic voltammetry (CV). To adsorb CO, the electrode was initially held in a CO saturated 0.1 M H_2SO_4 solution, at $E_{ads} = -0.65$ V for $t_{ads} = 3$ min.

The activity of dispersed Pt electrodes towards methanol oxidation was measured by CV in 0.1 M H_2SO_4 + 0.1 M CH_3OH. Several scans (−0.65 to 0.5 V

at $20\,mV\,s^{-1}$) were first applied. Voltammograms (-0.4 to $0.5\,V$ at $2\,mV\,s^{-1}$) were then recorded after that the potential was held at $-0.4\,V$ (MSE) for 3 min. The current intensity measured at 0 V (MSE) during the first forward scan, and corrected for the double layer charging contribution, allowed an evaluation of the specific activity (SA) and the mass activity (MA).

2.3. *TEM imaging*

The Pt deposits were imaged by TEM. The layer of carbon supported Pt and recast Nafion® was ultrasonically dispersed in ethanol. Then, a suspension in ethanol of the carbon powder supported Pt was deposited on a microscope grid coated with an amorphous carbon film. The grid was finally observed using a Jeol 100 CX microscope.

3. Results

3.1. *Electrochemical characterization of the carbon supports*

Typical layer thickness is about 5 μm, corresponding to carbon loading ranging from 340 to 565 $\mu g\,cm^{-2}$. Some of the cyclic voltammograms recorded for porous carbon electrodes are displayed in Fig. 1. For electrodes consisting of oxidized carbon powders, the CV reveals a wide anodic peak at about $-0.1\,V$ (MSE) and also, a wide cathodic peak at about $-0.2\,V$ (MSE), as shown in Fig. 1 curves (b) and (c). These peaks are attributed to the oxidation and the reduction of carbon surface oxide groups [28]. The chemical or electrochemical oxidation of carbon powders creates surface oxides consisting mainly of carboxylic and phenol groups [28, 29].

At $-0.5\,V$ (MSE), the measured current to mass ratio is about 0.6 to $2.0\,\mu A\,\mu g^{-1}$ for the as received and oxidized Vulcan powders, respectively, see Fig. 1 curves (a) and (b). These values, which characterize the double layer region, agree well with those reported for the same carbon black by Kinoshita [29]. For chemically oxidized HSAG powder, see Fig. 1 curve (c), the current to mass ratio is about $2.0\,\mu A\,\mu g^{-1}$. As the specific surface areas of the Vulcan and HSAG powders are 220 and $300\,m^2\,g^{-1}$, the double layer capacities of these porous electrodes are about 14, 45 and $33\,\mu F\,cm^{-2}$, respectively ($14\,\mu F\,cm^{-2}$ is a value close to that observed for a smooth electrode.)

3.2. *Evaluation of Pt deposit characteristics*

The quantity of electricity (Q_{tot} in $mC\,cm^{-2}$), used during the electrodeposition process at $-0.5\,V$, is calculated from the integral of the I/t transient response (Fig. 2). As the partial reduction of $PtCl_6^{2-}$ to Pt^{2+} species should occur at potentials more positive than $-0.3\,V$ (MSE) [30], and as the hydrogen evolution is negligible at $-0.5\,V$ (MSE), a current efficiency

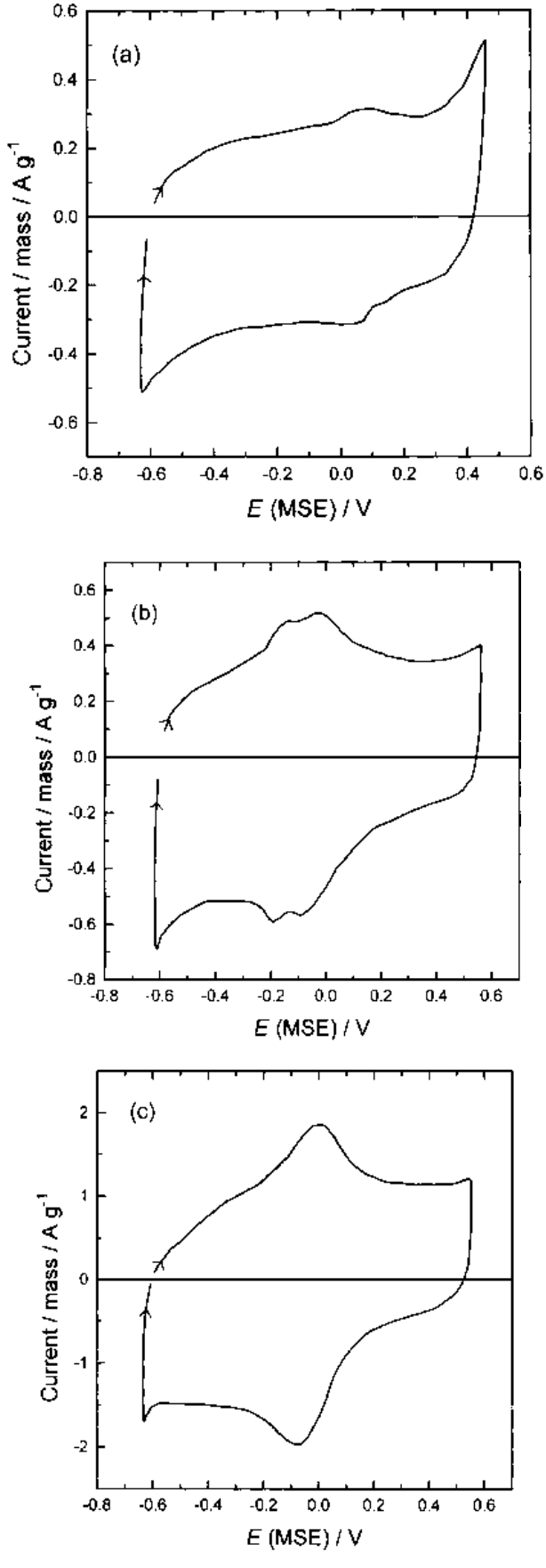

Fig. 1. Voltammogram recorded at $20\,mV\,s^{-1}$ in nitrogen-purged $0.1\,M\ H_2SO_4$ for a porous electrode of carbon powder and recast Nafion®. (a) As-received Vulcan XC72, carbon loading about $350\,\mu g\,cm^{-2}$, layer thickness about 4.0 μm. (b) Oxidized Vulcan XC72, carbon loading about $565\,\mu g\,cm^{-2}$, layer thickness about 6.5 μm. (c) Oxidized HSAG, carbon loading about $565\,\mu g\,cm^{-2}$, layer thickness about 6.5 μm.

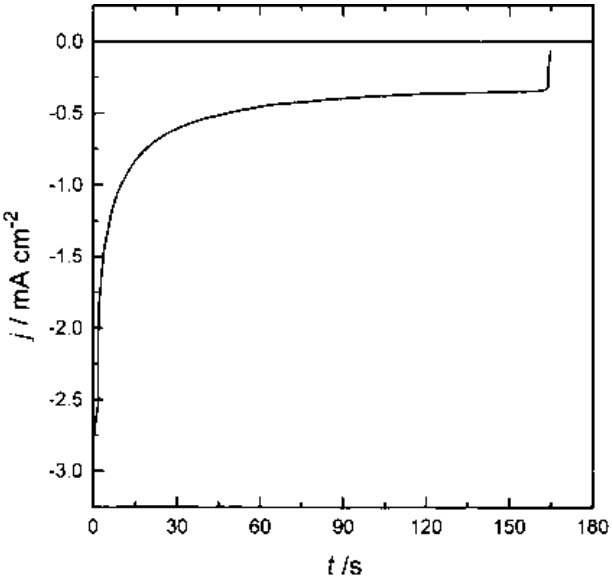

Fig. 2. Current against time response for a potential step from 0.05 to −0.5 V (MSE) in nitrogen-purged 0.1 M H_2SO_4 +2 mM K_2PtCl_6. Porous electrode consisting of HSAG graphite powder and recast Nafion®.

close to 100% is expected. Thus, the quantity of electricity (Q_{Pt} in mC cm^{-2}), resulting from the $PtCl_6^{2-}$ total reduction is

$$Q_{Pt} = Q_{tot} - Q_{dl} \quad (1)$$

where Q_{dl} in mC cm^{-2} is the quantity of electricity associated with the double layer charging and the reduction process of the surface oxides. The Q_{dl} values, which are listed in Table 1, are obtained by integration (between 0.05 and −0.5 V) of the I against $E(t)$ curves in the corresponding cyclic voltammograms (see Fig. 1). The Pt loading (W in μg cm^{-2}) is then

$$W = \frac{Q_{Pt}M}{zF} \times 10^3 \quad (2)$$

where $M = 195.1$ g mol^{-1} is the atomic weight of Pt, $z = 4$ the number of exchanged electrons and $F = 96\,500$ C mol^{-1}, the faradaic constant.

For oxidized carbon supports and under inert atmosphere, the H adsorption peaks are not clearly visible in the cyclic voltammogram. In contrast, for all the prepared electrodes, a sharp peak is visible beyond 0 V (MSE), during the first positive going scan following the adsorption of a CO layer. This peak, which corresponds to CO oxidation, is not observed during the second scan. Hence, at most one monolayer of CO is preadsorbed on the Pt surface. In addition, between −0.65 and −0.3 V (MSE), calculation of the quantities of electricity respectively involved when preadsorbed CO blocks the Pt surface (during the first scan) and after that CO was oxidized (during the second scan), allows an estimation of Q_H to be made, even for oxidized supports. Examples of such voltammograms are given in Fig. 3. The roughness factor (i.e., the ratio of the real to geometric surface area, γ in cm^2 cm^{-2}) is then calculated

Table 1. Electrochemical characteristics of the platinum electrodeposits

Sample	Q_{tot}/mC cm^{-2}	Q_{dl}/mC cm^{-2}	W/μg cm^{-2}	S/m^2 g^{-1}
Vulcan*	9.5	3.3	3	64
	24.0	2.3	11	38
	20.3	4.5	8	32
	66.3	2.5	32	19
Vulcan†	25.5	9.7	8	31
	88.2	10.1	39	15
HSAG	23.8	14.7	5	73
	36.5	23.3	7	37
	79.5	24.1	28	25

* As-received Vulcan
† Oxidized Vulcan

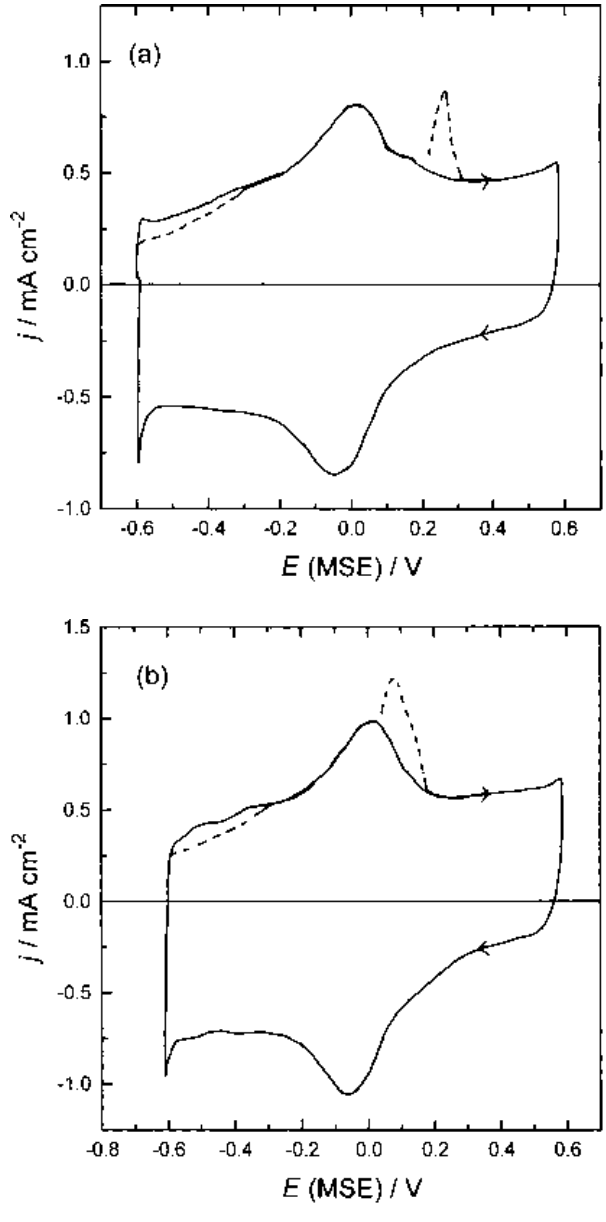

Fig. 3. Oxidation of preadsorbed CO recorded at 20 mV s^{-1} for an electrode of HSAG supported Pt and recast Nafion® immersed in nitrogen-purged 0.1 M H_2SO_4. Dotted line: 1st scan, solid line: 2nd scan. (a) Pt loading about 5 μg cm^{-2}; (b) about 28 μg cm^{-2}. Current density expressed in mA per unit of geometric surface area.

from H adsorption and CO oxidation coulometry (Q_H and Q_{CO} in mC cm^{-2})

$$\gamma = \frac{Q_H}{Q_H^0} \quad \text{or} \quad \gamma = \frac{Q_{CO}}{Q_{CO}^0} \tag{3}$$

with the theoretical quantities of electricity $Q_H^0 = 0.210$ and $Q_{CO}^0 = 0.420$ mC cm^{-2} of real Pt surface area [26, 27]. An average over all the prepared electrodes gives $Q_{CO}/Q_H = 2.0 \pm 0.3$. This calculated number of electrons per site agrees well with values previously obtained for a smooth Pt electrode [27]. It confirms that CO is linearly bonded to the Pt surface for long adsorption times (e.g., $t_{ads} = 3$ min) at cathodic adsorption potentials (e.g., $E_{ads} = -0.65$ V vs MSE), whatever the Pt surface morphology is.

Next, as both the Pt loading and the surface area are known, calculation of the specific surface area of Pt (S in m^2 g^{-1}) is given by

$$S = \frac{\gamma}{W} \times 10^2 \tag{4}$$

The calculated Pt loading and specific surface area are listed in Table 1. The S value increases from 15 to 73 m^2 g^{-1}, with W decreasing from 39 to 5 μg cm^{-2}.

The specific surface area is a useful macroscopic quantity to characterize the dispersed catalysts, but not to visualize the corresponding surface morphology. Using a simple structural model and fitting it to the specific surface area, assumptions for the surface morphology may, however, be derived and compared to the structural characterization of the corresponding electrode (e.g., by TEM observations). A simple model, considering the ideal situation, consists in assuming homogeneously distributed spherical particles. Accordingly, the characteristic particle diameter (d in nm) is related to the Pt specific surface area by:

$$d = \frac{6}{S\rho} \times 10^3 \tag{5}$$

where $\rho = 21.4$ g cm^{-3} is the density of Pt. The calculated particle diameters are listed in Table 2.

The TEM characterization of the prepared electrodeposits reveals heterogeneous distribution of Pt islands on the substrate surface. Numerous carbon pellets are observed, which show no Pt on their surface. On the other hand, when Pt electrodeposits are visible (the very dark spots in the micrographs, Fig. 4), they have the shape of very rough agglomerates consisting of several nanoparticles. Examples of such agglomerates are displayed in Fig. 4(a) and (b), for HSAG and Vulcan carbon supports, respectively. The Pt agglomerate size ranges typically from 10 to 50 nm, but smaller particles are also visible. The most striking observation is that, although the carbon supports are different, rather similar loading gives Pt deposits with almost the same feature.

3.3. *Methanol oxidation*

As shown in Fig. 5, for a given catalyst and from one forward-scan to the other, the peak potential of methanol oxidation ($E_{p,MeOH} \sim 0.1$ V) is not shifted. In addition, the measured current intensity is rather stable over two consecutive scans. This is explained by a reproducible distribution of adsorbed species on the Pt surface, at the beginning of each new scan.

Table 2. Specific activity SA and mass activity MA for methanol oxidation at 0 V (MSE) as a function of the Pt specific surface area

SA and MA are calculated from cyclic voltammograms recorded at 2 mV s^{-1} and room temperature in 0.1 M H_2SO_4 + 0.1 M CH_3OH

Sample	S/m^2 g^{-1}	d/nm[‡]	SA/μA cm^{-2}	MA/A g^{-1}
Vulcan[*]	64	4.5	37	24
	38	7.5	68	26
	32	9.0	75	24
	19	14.0	137	26
Vulcan[†]	31	9.0	126	39
	15	18.5	240	36
HSAG	73	4.0	67	49
	37	7.5	127	47
	25	11.0	196	49
E-TEK	112	2.5	41	46
bulk Pt	–	–	78	–

[*] As-received Vulcan
[†] Oxidized Vulcan carbon powder
[‡] Calculated assuming spherical Pt particles (see Eq. 5)

The calculated values of the specific activity and mass activity (SA and MA) are listed in Table 2. For the sake of comparison, an average value for a

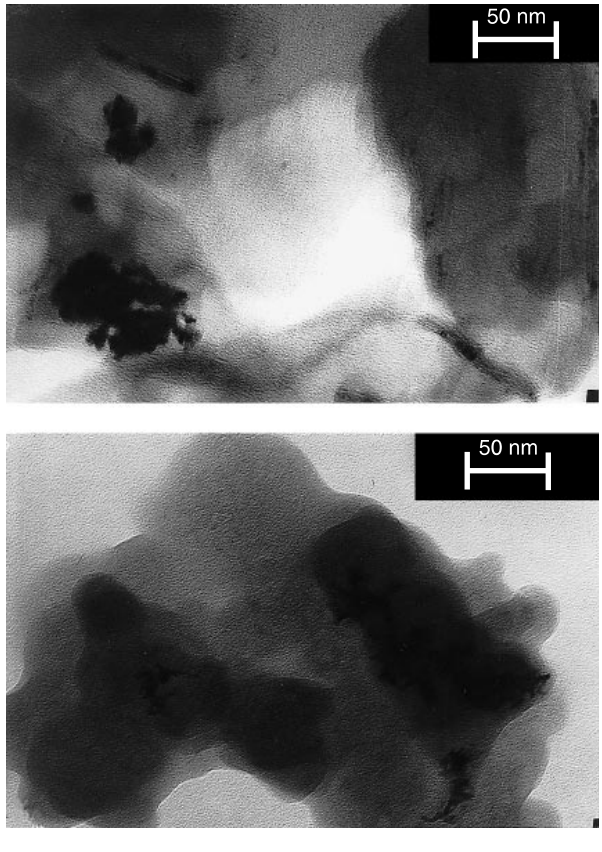

Fig. 4. TEM micrographs of Pt electrodeposits. (a) HSAG graphite support, Pt loading about 28 μg cm^{-2}; (b) as-received Vulcan carbon support, Pt loading about 32 μg cm^{-2}.

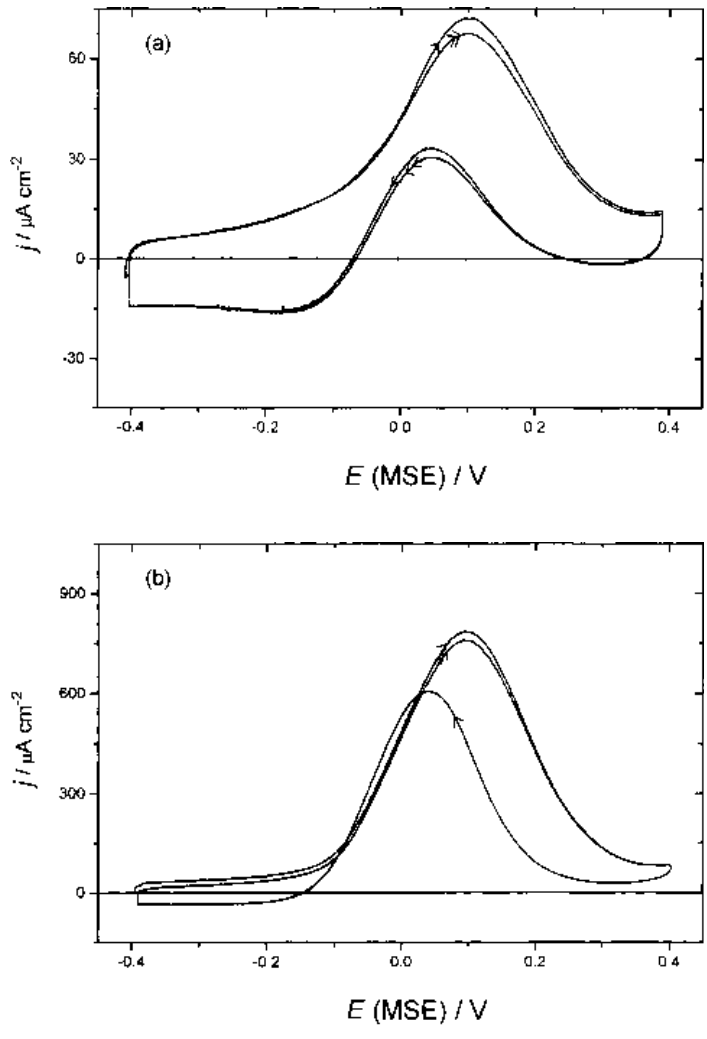

Fig. 5. Voltammogram recorded at $2\,mV\,s^{-1}$ in nitrogen-purged 0.1 M $H_2SO_4 + 0.1$ M CH_3OH for a porous electrode consisting of HSAG graphite powder and recast Nafion®. (a) Pt loading about $5\,\mu g\,cm^{-2}$, (b) about $28\,\mu g\,cm^{-2}$. Current density expressed in μA per unit of geometric surface area.

10 wt % Pt/Vulcan catalytic powder (E-TEK) and for bulk Pt are also included in Table 2. The results may be summarized as follows:

(i) At a similar Pt specific surface area (e.g., around $30\,m^2\,g^{-1}$), SA is greater for the oxidized than for the as-received Vulcan support, and the Pt electrodeposited on oxidized HSAG powder exhibits the best catalytic activities at any given specific surface area.
(ii) SA is divided by 3, as the Pt specific surface area increases by three times, independently of the carbon support.
(iii) SA is two or three times smaller for a smooth Pt electrode than for dispersed Pt electrodes with a Pt specific surface area around $20\,m^2\,g^{-1}$.
(iv) The mass activity does not depend on the Pt specific surface area. The average values are $MA = 49 \pm 1, 38 \pm 2$ and $25 \pm 1\,A\,g^{-1}$ for the HSAG, oxidized and as-received Vulcan powders, respectively.

4. Discussion

4.1. *Pt electrodeposition and characterization of the deposits*

As shown in Fig. 2, the I/t responses recorded in this work do not have the typical feature expected for a 3D nucleation process with diffusion control [31, 32]. Particularly, no rise in current with time indicates a nucleation process limited by spherical diffusion during the initial stage of nuclei growth. A multiple nucleation process may nevertheless occur, but its characterization is difficult, partly because of the high double layer capacity; the associated charging process may hinder the nucleation phenomena. Moreover, for such a characterization, $PtCl_6^{2-}$ diffusion through the porous electrode should be accounted for and simulated. As a first approach, the electrochemical data listed in Table 1 and the TEM imaging suggest nevertheless that the carbon surface structure and the amount of surface oxides have not a great effect on the Pt deposition process. This is in contrast to what was obtained for chemically reduced $PtCl_6^{2-}$ [33], *S*

decreasing with an increase of the amount of surface oxides. It was, however, also reported [19] that the specific surface area of Pt deposits depends on the specific surface area of carbon, and here the Vulcan and HSAG powders have almost the same specific surface area.

Since Nafion® is a cation exchange polymer, the concentration in $PtCl_6^{2-}$ at the carbon/Nafion® interface is low. Consequently, to achieve a significant Pt loading, the potential perturbation was applied for at least 30 s (corresponding to $W = 3$ and $5\,\mu g\,cm^{-2}$ in Table 1). For such a long time, the growth of the deposit is mainly controlled by the Pt salt diffusion in solution. Therefore, heterogeneous deposition through the porous layer is expected. This is confirmed, also not directly, by TEM observations. The lack of Pt deposits on many carbon pellets suggests that Pt is mainly deposited at the surface of the porous electrode. Short potential pulses should increase the specific surface area, and yield a more homogeneous distribution of Pt deposits. Nevertheless, to increase the Pt loading, the $PtCl_6^{2-}$ penetration through the porous electrode should be greatly enhanced. Experimental conditions which allow the Donnan potential difference to be overcome are presently under investigation.

TEM imaging shows that the Pt deposit morphology is far from the ideal model of homogeneously distributed spherical particles. Nevertheless, in respect of the so-called particle size effect, two factors have to be clarified:

(i) The sizes involved in the so-called particle size effect studies and estimated from direct measurements (SEM, TEM) are always average values. For most Pt/C powders, rather broad size distributions are observed, particularly when the particles are larger than 3 nm [34]. In addition, for particle size exceeding 5 nm, fine surface structures usually exist, which are not easy to characterize directly [35].

(ii) The average particle size may not be the only important parameter which must be related to the activity of carbon supported Pt. The particle shape (including the fine surface structure) and, in some cases, substrate effects, also have to be considered [36].

As a first approach, the Pt specific surface area, calculated from the electrochemically active surface area and the Pt loading, therefore seems to be the more convenient parameter in such studies. This macroscopic quantity (S) gives relevant information about the surface structure of dispersed Pt without making any assumption, averaging, or using any surface model.

4.2. *Methanol oxidation kinetics at the carbon supported Pt/Nafion® interface*

In this work, the observation of a large SA increase with a diminution of the Pt specific surface area is consistent with previous results [13] obtained under rather similar conditions for various Pt/C catalytic powders from E-TEK. In contrast, a SA decrease limited to specific surface areas greater than about $54\,m^2\,g^{-1}$ (i.e., for particles smaller than 5 nm) was reported by Frelink *et al.* [18]. However, the activity towards methanol oxidation was measured using voltammograms recorded from open circuit potential [18]. Since, in our work, the electrode was held at a cathodic potential, the Pt surface is therefore more strongly poisoned. This may explain the slight discrepancy between the results reported in [18] and those listed in Table 2.

Electrodeposited Pt (this work) and E-TEK catalysts [13] behave similarly, although the latter are supposed to consist of single particles with rather homogeneous size. The activity of Pt towards methanol electrooxidation thus seems mainly correlated to the fine surface structure of the dispersed catalyst. The relevance of a kinetic study, by using the catalysts prepared in this work, is therefore demonstrated.

In the course of methanol oxidation, dissociative chemisorption does occur [37]. Various intermediate species are formed, either weakly or strongly adsorbed. Some of these species act as poisons and further block the electrooxidation of methanol. The crucial step, which is generally accepted [20], is the oxidation of adsorbed intermediate species (coming from methanol) by oxygenated species (e.g., OH, OH_2) also adsorbed on the Pt surface. Three interpretations have thus to be considered to explain a particle size effect:

(i) Adsorption energy of the oxygenated species on the surface increases with the Pt specific surface area, so that the oxidation by oxygenated species of the adsorbed intermediates coming from methanol may become more difficult at a high Pt specific surface area.

(ii) The adsorption energy of the poisoning species may become stronger as the Pt specific surface area increases, in relation with a modification of the distribution of Pt sites.

(iii) The amount of initially adsorbed methanol may decrease as the Pt specific surface area increases, in relation with modifications of the surface structure of Pt particles [17, 18].

Due to the amount of surface oxides on the carbon supports, shifts of the peak potential, at which the reduction of oxygenated species does occur, cannot be accurately measured. During the backward-scan (i.e., at a fully oxidized Pt surface) and averaging over all the prepared Pt electrodeposits, the peak potential of methanol oxidation is $E_{p,MeOH} = 0.045 \pm 0.010\,V$ (MSE). In addition, according to Durand *et al.* [38], the reduction potential of the adsorbed oxygenated species under inert atmosphere and without methanol in solution was not greatly shifted ($-30\,mV$), for S ranging from 11 to $54\,m^2\,g^{-1}$. Since the Pt electrodeposits studied here (Table 2) are also in a medium range of specific surface area, the assumption

corresponding to a more difficult oxidation of the methanol intermediates by adsorbed oxygenated species, seems therefore unlikely.

The influence of a strong adsorption of poisoning species also has to be considered. Methanol oxidation is performed at initially poisoned Pt surfaces, but for the prepared Pt electrodeposits no significant shift of the potential of oxidation peak is observed during the first forward-scan, that is $E_{p,MeOH} = 0.100 \pm 0.020$ V (MSE). On the other hand, for bulk Pt and Pt/Vulcan (10 wt %, ETEK), $E_{p,MeOH} = 0.125 \pm 0.010$ and 0.080 ± 0.010 V (MSE), respectively. Thus, the potential of methanol oxidation is noticeably shifted in the negative direction with a Pt specific surface area increasing greatly (i.e., from a smooth surface to $S = 112\ m^2\ g^{-1}$); but at medium values of specific surface area, there is a poor effect of S on $E_{p,MeOH}$. Concerning preadsorbed CO oxidation, the peak potential is shifted from $E_{p,CO} = 0.050$ to 0.160 V (MSE), as the specific surface area of Pt electrodeposits increases from 25 to $73\ m^2\ g^{-1}$. This agrees well with $E_{p,CO} = 0.09$ and 0.18 V obtained respectively for bulk platinum and Pt/Vulcan (10 wt %, ETEK). As CO oxidation occurs when oxygenated species are adsorbed at the Pt surface [27], this large potential shift suggests that either CO or oxygenated species or both are much strongly adsorbed on highly dispersed Pt (see also Ref. [13]). This $E_{p,CO}$ shift agrees also with IR experiments [39] showing an increase of the adsorption energy of CO with the Pt specific surface area although these experiments were performed on roughened Pt and not on carbon supported Pt electrodes. Hence, from the peak potential measurements, it may be qualitatively concluded that, although 'CO-like' species are generally assumed to be the poisoning species produced in the course of methanol adsorption, the oxidation process of such poisoning species and preadsorbed CO cannot be directly compared. At present, any satisfactory explanation can be derived from the electrochemical data only. Our experimental results can be nevertheless discussed according to a recently published work. For the Pt(1 1 1) face in sulfuric acid solution, IRRAS and LEED measurements revealed that the $\theta_{bisulfate}/\theta_{CO}$ ratio is much greater in methanol than in CO containing solution. Beyond that, strong lateral interactions exist between bisulfate and adsorbed 'CO-like' species coming from the methanol dissociation [40]. Although sulfonate ions are a little weakly adsorbed than sulfate ions [25], similar lateral interactions between adsorbed sulfonate ions and adsorbed 'CO-like' species may occur. The strength of these interactions would be, of course, lower for dispersed Pt than for a smooth Pt surface, and therefore the poisoning would also be lower. This may explain that methanol oxidation occurs at more negative potentials on dispersed Pt, but also that the specific activity is greater for dispersed Pt electrodes than for bulk Pt electrodes (see Table 2 and [18]).

The last hypothesis, which has to be considered, is a possible modification of the distribution of methanol adsorption sites, with the specific surface area. This assumption is supported, but not directly, by experimental results on Pt single crystals [22, 23]. The catalytic activity is greatly affected by the Pt crystallographic structure. Initially (i.e., at a not poisoned surface), the (1 1 0) plane gives the highest activity for methanol oxidation, among the three low index planes. This was observed both for strongly and weakly adsorbed anions. A large specific activity for a dispersed Pt electrode may therefore be due to a high ratio of (1 1 0) crystal face on the Pt particle surface. However, the crystallographic structure of carbon supported Pt particles is difficult to determine experimentally.

The results listed in Table 2 show in addition, that the Pt specific activity increases with the amount of surface oxides on the carbon support. This observation agrees with already reported results [18, 19], and suggests metal support interactions. At a specific surface area lower than about $56\ m^2\ g^{-1}$ (i.e., in the case of Pt particle size larger than 5 nm), the amount of oxygenated species adsorbed at any given potential is not greatly modified by the Pt specific surface area [38, 18]. For a medium range of Pt specific surface area, as investigated in this work, the increase of the specific activity with the amount of carbon surface oxides seems likely related to the existence, on the carbon surface, of OH-like groups which are available for the oxidation of adsorbed intermediate species coming from the methanol dissociation. Electronic effects may also occur [33, 36], although in our opinion these effects should be detected only for very small particles (~1 nm in size).

5. Conclusion

The results of this work may be summarized as follows:

(i) TEM observations reveal an heterogeneous distribution of electrodeposited Pt through a porous electrode consisting of carbon powder plus recast Nafion®. However, the resulting morphology of the Pt particles is not greatly modified neither by the structure of the carbon support, nor by the amount of carbon surface oxides.

(ii) Both the Pt mass and specific activity (*MA* and *SA*) for methanol oxidation increase with the amount of surface oxides on the carbon support.

(iii) Although the particle size cannot be directly estimated from TEM observations, *SA* decreases significantly with increasing Pt specific surface area. Moreover, *MA* depends on the carbon structure only, and not on the Pt specific surface area.

(iv) The catalytic activity of a smooth Pt electrode toward the methanol oxidation is much lower than that calculated for slightly dispersed Pt electrodes.

It had already been reported [13] that smooth and slightly dispersed Pt electrodes have the same activity for the ORR, and that the ORR kinetics does not depend on the crystallographic structure of the Pt surface [23]. Hence, in the case of the ORR, the Pt catalytic activity seems to be directly related to the Pt particle size. In contrast, the experimental results obtained in this work for the methanol oxidation suggest that the Pt activity is not directly related to the particle size, but more likely to the fine structures of the Pt surface (see experiments on Pt single crystals [21, 22, 40]). The fine structures of the dispersed Pt surface may depend, their turn, on the Pt specific surface area, on the nature of substrate or on the preparation procedure of the catalyst.

Acknowledgements

This work was carried out with the support (contract 3.91.0013) of ADEME, the French Agency for Environment and Energy Conservation, to which we are greatly indebted.

References

[1] B. Beden, J. M. Léger, and C. Lamy, *in* 'Modern Aspects of Electrochemistry', Vol. 22 (edited by J. O'M. Bockris, B. E. Conway and R. E. White), Plenum Press, New York, (1992), p. 97.
[2] J. B. Goodenough, A. Hamnett, B. J. Kennedy, R. Manoharan and S. A. Weeks, *Electrochim. Acta* **35** (1990) 199.
[3] M. P. Hogarth, J. Munk, A. K. Shukla and A. Hamnett, *J. Appl. Electrochem.* **24** (1994) 85.
[4] X. Ren, M. S. Wilson and S. Gottesfeld, *J. Electrochem. Soc.* **143** (1996) L12.
[5] E. Tricianelli, C. R. Derouin, A. Redondo and S. Srinivasan, *ibid.* **135** (1988) 2209.
[6] E. J. Taylor, E. B. Anderson and N. R. K. Vilambi, *ibid.* **139** (1992) 145.
[7] M. W. Verbrugge, *ibid.* **141** (1994) 46.
[8] R. Le Penven, W. Levason and D. Pletcher, *J. Appl. Electrochem.* **22** (1992) 415.
[9] K. Itaya, H. Takahashi and I. Ushida, *J. Electroanal. Chem.* **208** (1986) 373.
[10] J.-H. Ye and P. Fedkiw, *Electrochim. Acta* **41** (1996) 221.
[11] S. Mukerjee, *J. Appl. Electrochem.* **20** (1990) 537.
[12] K. Kinoshita, *J. Electrochem. Soc.* **137** (1990) 845.
[13] A. Kabbabi, F. Gloaguen, F. Andolfatto, and R. Durand, *J. Electroanal. Chem.* **373** (1994) 251.
[14] A. Gamez, D. Richard, P. Gallezot, F. Gloaguen, R. Faure, and R. Durand, *Electrochim. Acta* **41** (1996) 307.
[15] P. A. Atwood, B. D. McNicol, and R. T. Short, *J. Appl. Electrochem.* **10** (1980) 213.
[16] M. Watanabe, S. Saegusa and P. Stonehart, *J. Electroanal. Chem.* **271** (1989) 213.
[17] K. Yahikozawa, Y. Fujii, Y. Matsuda, K. Nishimura and Y. Takasu, *Electrochim. Acta* **36** (1991) 973.
[18] T. Frelink, W. Visscher and J. A. R. van Veen, *J. Electroanal. Chem.* **382** (1995) 65.
[19] M. Uchida, Y. Aoyama, M. Tanabe, N. Yanagihara, N. Eda and A. Ohta, *J. Electrochem. Soc.* **142** (1995) 2572.
[20] R. Parsons and T. VanderNoot, *J. Electroanal. Chem.* **257** (1988) 9.
[21] C. Lamy, J-M Léger, J. Clavilier and R. Parsons, *ibid.* **150** (1983) 71.
[22] B. Bittings-Cattaneo, E. Santos and W. Vielstich, *Electrochim. Acta* **31** (1986) 1495.
[23] F. El Kadiri, R. Faure and R. Durand, *J. Electroanal. Chem.* **301** (1991) 177.
[24] F. Gloaguen, F. Andolfatto, R. Durand and P. Ozil, *J. Appl. Electrochem.* **24** (1994) 863.
[25] E. Yeager, M. Razaq, D. Gervasio, A. Razaq and D. Tryk, *in* 'Structural Effects in Electrocatalysis and Oxygen Electrochemistry', The Electrochemical Society, Pennington NJ, **PV 92–11** (1992), p. 140.
[26] T. Biegler, D. A. J. Rand and R. Woods, *J. Electroanal. Chem.* **29** (1971) 269.
[27] B. Beden, C. Lamy, N. R. De Tacconi and A. J. Arvia, *Electrochim. Acta* **35** (1990) 691.
[28] K. Kinoshita, 'Carbon: Electrochemical and Physicochemical Properties', Wiley-Interscience, New York (1988), p. 299.
[29] A. Tomita and Y. Tamai, *J. Phys. Chem.* **75** (1971) 649.
[30] K. Shimazu, D. Weisshaar and T. Kuwana, *J. Electroanal. Chem.* **223** (1987) 223.
[31] J. Lin Cai and D. Pletcher, *J. Electroanal. Chem.* **149** (1983) 237.
[32] B. Scharifker and G. Hills, *Electrochim. Acta* **28** (1983) 879.
[33] P. L. Antonucci, V. Alderucci, N. Giordano, D. L. Cocke and H. Kim, *J. Appl. Electrochem.* **24** (1994) 58.
[34] E. A. Ticianelli, J. G. Beery and S. Srinivasan, *ibid.* **21** (1991) 597.
[35] K. Shimazu, K. Uosaki, H. Kita and Y. Nodasaka, *J. Electroanal. Chem.* **256** (1988) 481.
[36] O. Savadogo, *in* 'Proceedings of the First International Symposium on New Materials for Fuel Cell Systems' (edited by O. Savadogo, P. R. Roberge and T. N. Veziroglu), Editions de l'Ecole Polytechnique de Montréal, (1995), p. 544.
[37] M. I. S. Lopes, B. Beden, F. Hahn, J. M. Léger, and C. Lamy, *J. Electroanal. Chem.* **313** (1991) 324.
[38] R. Durand, R. Faure, F. Gloaguen, and D. Abberdam, *in* 'Symposium on Oxygen Electrochemistry', The Electrochemical Society, Pennington NJ, **PV 95–26** (1995), p. 27.
[39] B. Beden, F. Hahn, C. Lamy, J-M. Léger, N. R. De Tacconi, R. O. Lezna and A. J. Arvia, *J. Electroanal. Chem.* **261** (1989) 401.
[40] H. Ogasawara and M. Ito, *Chem. Phys. Lett.* **245** (1995) 304.